Kurdish Studies
August 2024
Volume: 12, No: 4, pp 1719 -1731
ISSN: 2051-4883 (Print) | ISSN 2051-4891 (Online)
www.KurdishStudies.net

DOI: 10.53555/ks.v12i4.3614

Transition of Flow Past Five Square Obstacles in Tandem Arrangement at Distinct Gap Spacing

Raheela Manzoor[1]*, Shazia Kalsoom[1], Tyyaba Kalsoom[3], Farida Panezai[2], Neelam Panezai[1], Naveed Sheikh[4], Muhammad Yasin[2]

[1]Mathematics Department, SBK Women's University, Quetta, Balochistan, Pakistan.
[2]Mathematics Department, BUITEMS, Balochistan, Pakistan.
[3]Computer science Department, National University of Technology, Pakistan.
[4]Mathematics Department, University of Balochistan, Pakistan.

***Corresponding Author:** Raheela Manzoor
*Email: raheela_manzoor@yahoo.com

Abstract:
A two-dimensional (2-D) numerical simulation was performed for the flow past five square obstacles of similar size 'D' aligned inline at fixed Reynolds number Re = 150 to investigate the transition in flow behavior. The gap spacing (gc = s/D) between the obstacles was varied from gc = 0.25 to 5. The results were obtained in terms of vorticity contour visualization, time-history analysis of drag (Cd) and lift (Cl) forces, and physical parameters. Four different flow modes were identified under the effect of gap spacing (gc = s/d). These are: i) Shear layer flow mode ii) Half-developed irregular vortex shedding flow mode iii) Fully-developed two-row vortex shedding flow mode iv) Two-row single bluff body flow mode for obstacles C1-C5. The values of Cdmean, Cdrms, Clrms, and St were calculated for physical parameters. Cdmean exhibited a mixed trend with increasing gap spacing for obstacles C3, C4, and C5. The highest value of Cdmean was observed at gc = 5 for obstacle C1, which was 1.4594, while the smallest value was attained for obstacle C3 at gc = 0.25. There were also some negative values of Cdmean for obstacle C2 at gc = 0.25 - 2.25 and for obstacle C3 at gc = 0.25 - 1.25 due to the effect of pressure, known as thrust. Furthermore, the Strouhal number showed an increasing trend for both small and large gap spacings, i.e., gc = 0.25 - 0.75 and gc = 1.5 – 5. The highest value of the Strouhal number was observed at gc = 5 for obstacle C5, which was 0.1521.

Keywords: Drag and lift coefficients, Steady flow, Force statistics, square obstacles, Gap spacing.

1. Introduction

Fluid Flow around single or multiple objects in different configurations such a tandem, side by side and staggered arrangements have been observed in various filed of engineering, such as chimneys, cooling devices, micro-electro-mechanical systems, construction of buildings and bridges etc. These structures are faced by fluid-induced forces, when they interacted with fluids like air or water. Therefore, it is important to investigate the resulting effects of their interaction, which may be related to structural vibration phenomenon. Many studies are available in literature to investigate the structural vibration phenomena by using more than one objects of similar diameters that may be circular/rectangular or square [Hishikar et al.., (2001), Bovand et al., (2016), Salwa et al., (2021), Salwa et al., (2020) and Salwa et al., (2018)]. Zhou et al., (2006) performed an experiment for study the flow structure mechanism and heat transfer in between the region of two tandem circular obstacles by using gap spacing from g_c = 1.3 to 6 at Re = 7000. They examined four distinct types of flow mods. Sohankar and Etminan (2009) numerically studied the phenomena of forced convection heat transfer in laminar flow past tandem square obstacles at Re = 1 - 200. They studied the effects of Reynolds number on flow mechanism and heat transfer at fixed value of gap spacing. Xu and Zhou (2004) experimentally measured the S_t values for flow past two circular obstacles by taking the range of Reynolds number from 800 to 4.2×10^4 and g_c = 1 to 15 for tandem arrangement. They examined critical gap spacing within the range from g_c = 3.5 to 5. Liu and Chen (2002) experimentally studied flow past over tandem square obstacle at Re = 2000 - 16000 and examined two various types of flow mods by progressively increasing and decreasing the gap spacing from g_c = 1.5-9. Sohankar (2011) numerically examined the influence of gap spacing for flow past two tandem square obstacles by taking g_c = 3 – 12 at Re = 130, 150 and 500. They notified three different types of flow mods. Inoue et al., (2006) carried out numerical study for flow past two tandem square obstacles for the sound generation in a uniform flow at low Mach number with Re = 150. Liu (2003) performed numerical study for flow past one-, two-, three- and four tandem circular obstacles of identical diameter and found the critical gap spacing between g_c = 3.5 and 4 for Re ranging from 27,000 to 86,000. He found a sharp increase in drag coefficient for middle and downstream obstacles at critical value of g_c. Tatsutani et al., (1993) performed numerical simulations for two tandem square obstacles in a channel for Re ranging between 200 to 1600. They observed distinct flow mods that are dependent on a critical inter-obstacle spacing. An experimental study on the flow characteristics around three circular obstacles is conducted by Igrashi and Suzuki (1984) and divided the flow behavior in three types. (i) without reattachment, (ii) with reattachment and (iii) rolling up. Moreover, they examined that drag force of central obstacle was negative for the spacing values g_c < 3.53. Harichandan and Roy (2010) numerically examined the flow over three inline circular obstacles at Re = 100 and 200 at different values of g_c and found that the obstacle placed at downstream location was

experienced huge amount of unsteady forces that caused the damaging of the structure. At Re = 100 and g_c = 2, they observed steady flow mod. An experimental study was conducted by Lam and Lo (1992) for the flow past over four obstacles at different values of gap spacing in the range g_c = 1.28 -5.96 and Re = 2.1 × 10^2 through induced fluorescent visualization. They examined three different flow modes. A (2-D) numerical study is conducted for flow past an inline configurations of square obstacles by Patil and Tiwari (2009) to find out the behavior of flow field at different ranges of g_c and Re. They found vortex shedding suppression at value of g_c greater than 1. The Cd_{mean} of first obstacle contained positive and end obstacle was attained negative values because of increasing the values of gap spacing. A numerical simulation for flow past over four square obstacles through LBM to study the effect of spacing ratio at Re = 150 was done by Abbasi et al., (2014). They investigated four different types of flow mods depending on value of gap spacing. Lam and Zhou (2007) studied the flow behavior past over the four circular obstacles in an inline square arrangement at different values of g_c from 1.5 to 5 and Reynolds number was varied from 1.128 × 10^4 to 1.982 × 10^4. The flow past over five inline circular obstacle experimentally examined by Hetz et al., (1991) at Reynolds number in the range Re = 1 × 10^4 to 5 × 10^4. They identified various flow structures at different values of Re and g with dominancy of one flow mod over other. Sewatkar et al., (2012) numerically as well as experimentally investigated the flow around six inline square obstacles to study the flow mode at some selected values of g_c and Re. that are 0.5 ≤ g_c ≤ 10 and 80 ≤ Re ≤ 320. They investigated the negligible influence in average Cd_{mean} of first obstacle due to presence of other two obstacles. The flow past over six square obstacles in tandem configuration at the spacing range 1.5 ≤ g_c ≤ 15 and Re = 100 is numerically examined by Bao et al., (2012) and six different types of flow mods were found in their investigations.

From above mentioned literature, it is cleared that no more attention was paid to study the flow past more than four objects in tandem arrangement. No work in literature was reported on the influence of gap spacing for five tandem square obstacles at constant value of Reynolds number i.e. Re = 150. By keeping focus on these points, the present study was based: (i) to investigate the effects of spacing ratio for the flow past five square obstacles aligned in-line at Re = 150 (ii) to examine the variation of flow mod in wake region and outside the wake region in the whole computational domain, iii) to study the physical parameters with respect to change in spacing ratios and (iv) to study the applications of lattice Boltzmann method for flow past over the complicated fluid flow problem. These points will be discussed in the following sections in detail.

2. Lattice Boltzmann Method

Lattice Boltzmann method is a numerical approach used to solve simple or complex fluid flow problems over the last few decades. It was derived by LGCA (Mohammad (2011)) and firstly introduced in 1988 by Mac-Namara and Zanetti (1988). LBM has become a most important technique for solving fluid flow problems, due to its easy execution, parallel computing system and ability to handle complicated and complex geometries, it has become a prevalent technique for evaluating simple and complex fluid flow problems (Wolf-Gladrow (2005)). Additionally, the pressure is a local variable in Lattice Boltzmann Method and there is no use of Poisson equation to solve for finding the pressure (Mohammad (2011)). We can compute pressure through equation of state ($p = \rho c_c^2$). The LBM is based on the famous Lattice Boltzmann Equation (LBE):

$$h_i(\mathbf{x} + \mathbf{c_i}, t + 1) = h_i(\mathbf{x}, t) + \Omega_i(\mathbf{x}, t) \quad (1)$$

where $h_i(\mathbf{x}, t)$ is the density distribution function that indicates the position **x** of a particle at time t, **c** is the velocity of the particle and Ω is the collision operator. Using the Bhatnagar-Gross-Krook (BGK) collision operator, the discretized form of the above equation is given by Bhatnagar-Gross-Krook (1954),

$$h_i(\mathbf{x} + \mathbf{c_i}, t + 1) = h(\mathbf{x}, t) - 1/\tau[(h_i(\mathbf{x}, t) - h_i(\mathbf{x}, t)] \quad (2)$$

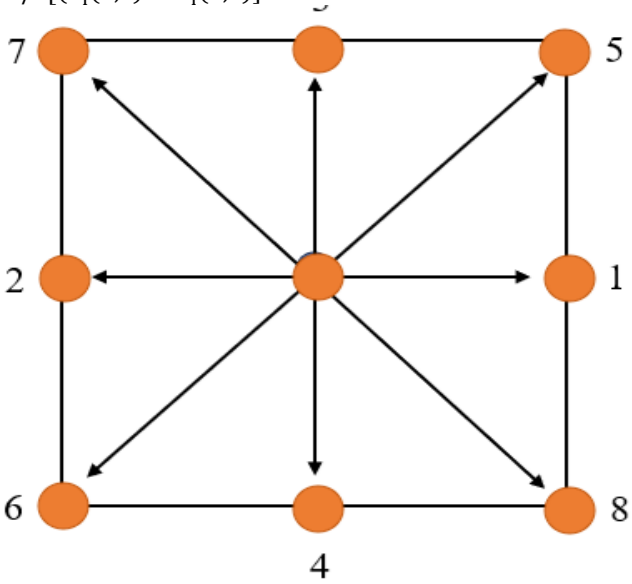

Fig 1. Two dimensional nine particle velocity model (d'Humieres (1992)).

Where τ is the single relaxation time and to control stability of method, whereas $h_i(x, t)$ and $h_i^{eq}(\mathbf{x}, t)$ is density distribution and the equilibrium distribution function (EDF) given by Lam and Zhou (2007),

$$h_i^{eq} = \xi_i \eta \left[1 + \frac{\mathbf{c_i}.\mathbf{u}}{c_s^2} + \frac{(\mathbf{c_i}.\mathbf{u})^2}{2c_s^4} - \frac{\mathbf{u}^2}{2c_s^2}\right] \quad (3)$$

LBM based on different structure or model, but most commonly used model is D2Q9 (where D is represented the dimensions and Q represented the number of particles) (see Fig 1). We are also using this model for present problem. (d'Humieres (1992)). The weighting coefficients for D2Q9 model are, $\xi_r = 4/9$ for r = 0, $\xi_S = 1/9$ for s = 1, 2, 3, 4 and $\xi_L = 1/36$ for l = 5, 6, 7, 8, respectively. The discrete velocity set $\{e_i\}$ is written as $e_0 = (0,0)$, $e_{i,3} = (\pm 1, 0)$, $e_{2,4} = (0, \pm 1)$, and $e_{5,6,7,8} = (\pm 1, \pm 1)$. Moreover, $c_s = 1/\sqrt{3}$ is the speed of sound and used to find the kinematic viscosity, $\gamma = (\tau - 0.5)c_s^2$.

3. Geometry of problem and boundary conditions

The geometry of present problem is based on flow past five square obstacles aligned inline of similar sizes 'D' as shown in Fig 2. The values of gap spacing is varied from g_c = 0.25 to 5 at fixed value of Re = 150. Obstacle C_1 is the upstream obstacle placed at L_u = 6D from the inlet position, while obstacle C_5 is the obstacle placed at last position. The distance from C_5 to exist position of channel is called downstream position is denoted by L_d and taken as L_d = 25D. While the other three obstacles C_2, C_3 and C_4 are put in between the upstream and downstream obstacles. The height of channel is fixed at H = 11D and its length varies by varying the spacing ratios between the obstacles as shown in Table 1. Uniform inflow velocity condition $(\mathbf{u} = U_\infty; \mathbf{v} = 0)$ is used at inlet, where U_∞ is inflow velocity along x- direction and **v** = 0 is shown that there is no flow in y-direction. The convective boundary condition $((\frac{\partial \mathbf{u}}{\partial \mathbf{t}} + \mathbf{U}_\infty \frac{\partial \mathbf{u}}{\partial \mathbf{x}} = 0))$ is applied at the outlet position of the channel (Guo (2008)).

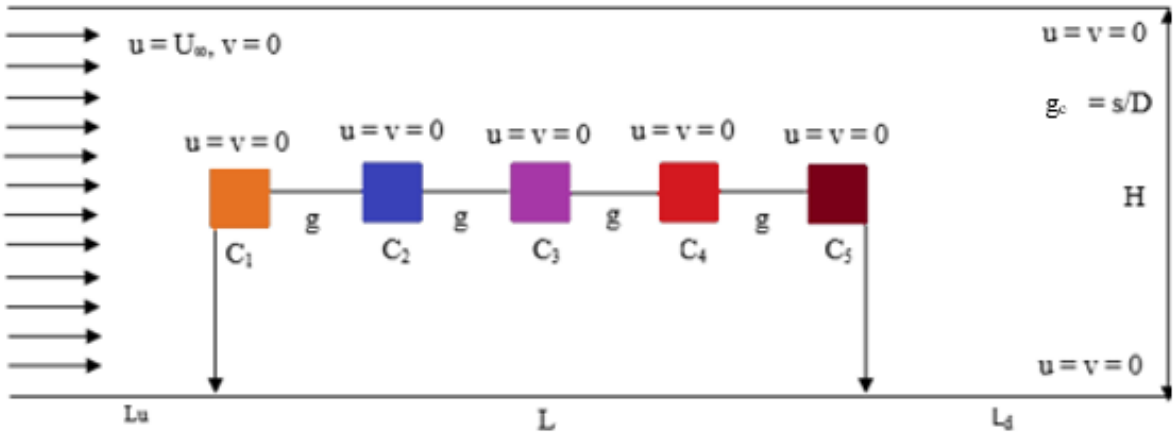

Fig 2. Schematic diagram for the flow past five in-line square obstacles.

Due to stationary position of obstacles, no-slip condition (**u = v =** 0**)** is also used at the walls of the obstacles as well at the top and bottom walls of the channel (Yu et al., (2003)). The total forces of fluid on the square obstacle are calculated through the momentum exchange method (Yu et al., (2003)). In the present problem by using the LBM, we used the value of uniform velocity U_∞ = 0.04385964 for getting reasonably good results at τ = 0.526315784 for Re = 150 and D = 20. The code for present study was written and edited using Compaq Visual Fortran version 6.5.0. All selected cases for present simulation are shown in Tab. 1.

Table 1. Selected cases for simulation of present study at Re = 150.

Cases	L × H	Cases	L × H
g_c = 0.25	741× 221	g_c = 2.5	921 ×221
g_c = 0.5	761× 221	g_c = 2.75	941 ×221
g_c = 0.75	781× 221	g_c = 3	961 ×221
g_c = 1	801× 221	g_c = 3.25	981× 221
g_c = 1.25	821× 221	g_c = 3.5	1001 ×221
g_c = 1.5	841 ×221	g_c = 3.75	1021× 221
g_c = 1.75	861 ×221	g_c = 4	1041× 221
g_c = 2	881 ×221	g_c = 5	1121× 221
g_c = 2.25	901× 221		

4. Code validation and grid independence study

In order to find the adequate grid points for present problem, the developed code is checked by considering 10D, 16D, 20D, 24D, 30D and 40D points along the surface of obstacle. The physical parameter Cd_{mean}, Cd_{rms}, Cl_{rms} and S_t are computed at Re = 150 as shown in Tab 2. X ×Y = 321 × 111 points are used in x, y directions, respectively, for 10D, 513 ×177 points used for 16D, 641 × 221 points used for 20D, 768 × 265 points used for 24D, 961 × 331 for 30D and 1281 × 441 used for 40D, respectively in **x**, **y** directions. It is noticed from the table that the data obtained from the 20D grid points gives accurate results to meet convergence criteria as compared to 10D, 16D, 24D, 30D and 40D grid points. Therefore, whole simulations are done by using 20D grid points for present problem.

Table 2. Comparison of physical parameters at various grid points for Re = 150.

Re = 150	**10D**	**16D**	**20D**	**24D**	**30D**	**40D**
Cd_{mean}	1.307 (2.43%)	1.276 (0.08%)	1.275 (1.03%)	1.262 (0.56%)	1.255 (3.46%)	1.213
Cd_{rms}	0.0199 (19.2%)	0.0167 (3.73%)	0.0161 (5.9%)	0.0152 (4.11%)	0.0146 (6.6%)	0.0137
Cl_{rms}	0.304 (12.1%)	0.271 (2.65%)	0.264 (2.32%)	0.258 (1.18%)	0.255 (1.63%)	0.2509
S_t	0.1756 (8.7%)	0.1615 (1.44%)	0.1592 (6.5%)	0.1494 (6.9%)	0.1369 (1.94%)	0.1343

In order to validate our numerical code for current study, we have calculated the values of physical parameters like Cd_{mean} and S_t for flow past a SSR (Single square obstacle) at Re = 100, 150, 175 and 200. The numerical technique is validated by comparing the obtained results from current simulation with other available data in literature for the flow around a SSR as described in Table 3, where Exp representing the experimental work and num is representing the numerical work.

Table 3. Study of code validation for flow past a SSR at Re = 150

	Cd_{mean}				**S_t**			
Re	**100**	**150**	**175**	**200**	**100**	**150**	**175**	**200**
Present	1.484	1.493	1.524	1.572	0.149	0.154	0.165	0.149
Okajima (1982) **exp**	1.60	1.492	1.482	1.480	0.141	0.142	0.140	0.138
Davis &Moore (1982) **exp**	1.64	------	-------	1.72	0.1482 0	------	------	0.1470
Malikzadeh & Sohankar (2012**) num**	1.444	1.408	1.412	1.424	0.145	0.161	0.165	0.163
Robichaux et al., (1999**) num**	1.54	1.56	1.60	1.63	0.154	0.164	0.158	0.156
Gera & Sharma (2010) **num**	1.461	1.411	1.472	1.487	0.129	0.141	0.143	0.143
Abograish & Alshayii (2013) **num**	1.485	1.474	1.483	1.488	0.140	0.1528	0.1528	0.1528

It can be examined that Cd_{mean} and values of Strouhal number are shown a good agreement with the experimental as well as numerical values available in literature. This indicated that the present code can simulate the flow characteristics in an efficient manner. There may be observed some minute differences in between the calculated values and available data from literature at Re = 100, 175 and 200 due to use of different numerical techniques, boundary conditions as well use of different grid points. The comparison of Cd_{mean} for flow past two, three, four and five obstacles aligned inline is described in Tab. 4.

Table 4. Comparison of Cd_{mean} for flow past two, three, four and five obstacles aligned inline.

Single Obstacle	**Two inline arrangement**					
	Cd_{mean}	Cd_{mean} 1	Cd_{mean} 2	----------		
	1.340	1.2892	1.0126	----------		
% Reduction Cd_{mean}		3.8%	24.43%	----------		
	Three inline arrangement					
	Cd_{mean}	Cd_{mean} 1	Cd_{mean} 2	Cd_{mean} 3	----------	
	1.340	1.2503	-0.0836	0.2184	----------	
% Reduction Cd_{mean}		6.7%	106.23%	83.7%	----------	
	Four inline arrangement				---------	
	Cd_{mean}	Cd_{mean}1	Cd_{mean}2	Cd_{mean}3	Cd_{mean}4	
	1.340	1.491 (49.1%)	1.123 (16.19%)	0.093 (93.1%)	0.122 (87.8%)	
% Reduction Cd_{mean}	**Five inline arrangement**					
	Cd_{mean}	Cd_{mean}1	Cd_{mean}2	Cd_{mean}3	Cd_{mean}4	Cd_{mean}5
	1.340	1.454	0.8546	0.0364	0.1115	0.2203
% Reduction Cd_{mean}		8.5%	36.2%	97.3%	91.7%	83.6%

5. Results and discussions

A (2-D) numerical study is carried out for flow past five inline square obstacles of same sizes (D) at constant value of Re = 150. The gap spacing is chosen between the obstacles from g_c = 0.25 – 5. The flow structure mechanism is analyzed in terms of vorticity, time-history analysis of drag and lift coefficients and force statistics.

5.1. Analysis of Vorticity contour and drag and lift coefficients

In this section, the existing flow mods from g_c = 0.25 – 5 and their drag and lift coefficients are discussed briefly at Re = 150 for sake of simplicity and repeated results are avoided to show here.

5.1.1. Share layer reattachment flow mod (SLR)

This flow mod is observed at g_c = 0.25-1.75 as shown in Fig 3(a-d). Where the generated shear layer after hitting the obstacle, separated into two layers, first one is moved to upside of the obstacle and other one moved towards the downside of the obstacles. These two layers are reattached directly at downstream location of channel after splitting from obstacles, so called SLR flow mod. At g_c = 0.25 and 0.5, due to narrow space, no flow interaction is observed in between the obstacles, but by increasing g_c from 0.75 to 1.75, symmetric flow behavior is found in between the gap. An alternate vortex shedding is examined towards the downstream of obstacles in the form of von-Karman Vortex Street. A slight modulation in the flow behavior is occurred at g_c =1.75 as compared to g_c = 0.25 - 1.5 due to this recirculation zone observed behind the obstacle C_4. The shape of vortices became more prominent with large gap spacing and there is a variation in the shape and size of the vortices with increase in gap spacing. The width of wake region also varied to some extent with increment in values of gap spacing.

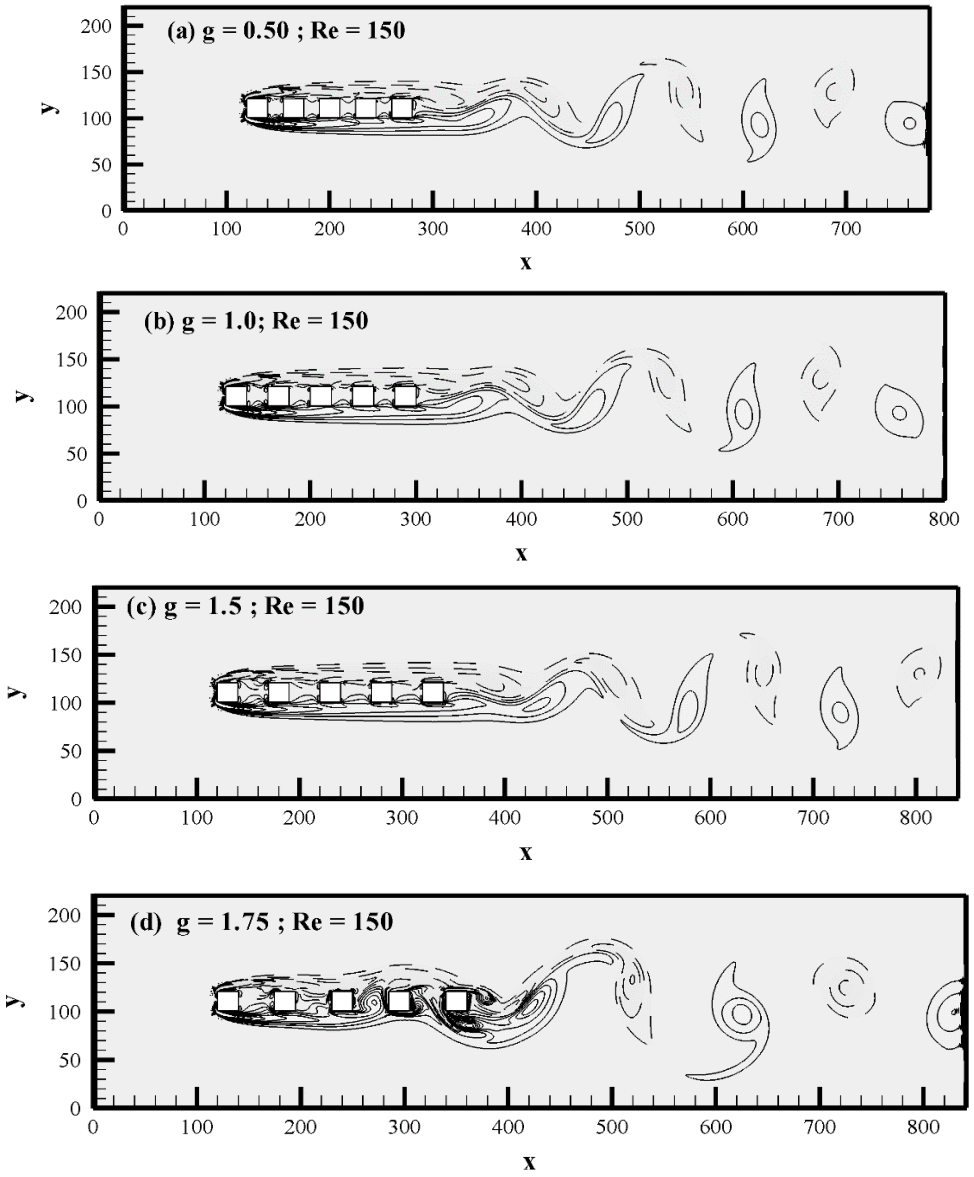

Fig 3(a-d). Vorticity contour for SLR flow mod.

The drag coefficient of fluid force is confirmed that there is no flow existed between the obstacles and constant drag force are exerted by the flow on obstacles as shown in Fig 4(a-h). It can be noticed that drag force of obstacle C_2 is negative. This is due to the fact, that the spacing between the obstacles is narrow and strong suction is created in the gaps. As a result, drag force became negative. The magnitude of Cd for obstacle C_1 is maximum and minimum for obstacle C_2. The lift coefficients is represented the periodic behavior due to an alternate vortex shedding at downstream location and the behavior of vortices remain almost same at downstream location of obstacles (see Fig. 3). The amplitude of Cl is increased with the increment in gap from g_c = 0.25 to 1.75. In comparison of all five selected obstacles, obstacle C_5 having largest and obstacle C_1 is contained smallest amplitude of lift coefficients.

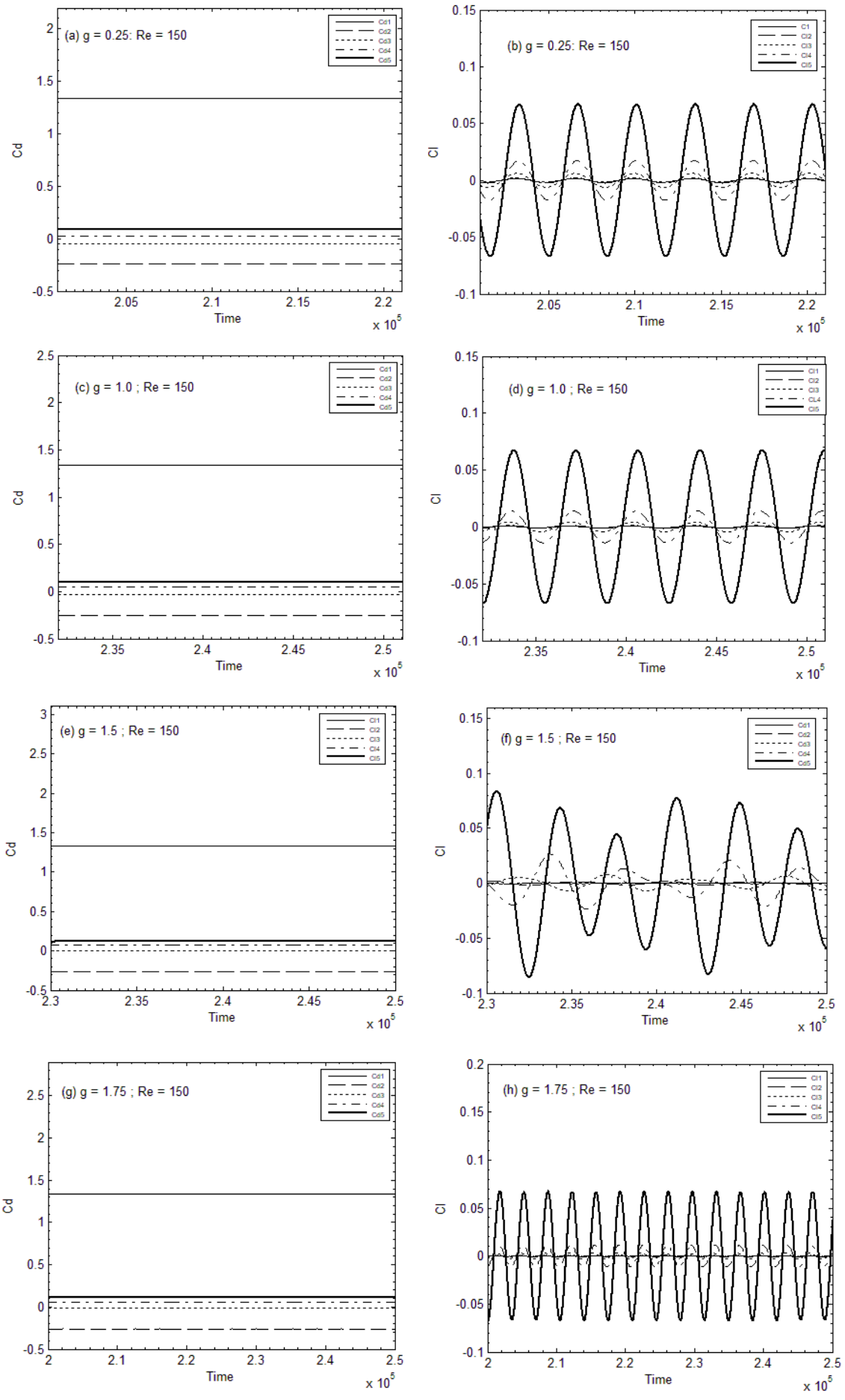

Fig 4(a-h). Drag and lift coefficients for SLR flow mod.

5.1.2. Half-developed irregular vortex shedding flow mod

The second existing flow mod is named as HDIVS (Half developed irregular vortex shedding) flow mod, observed only at g_c = 2.0 and 2.25 at Re = 150. In this flow mod, no flow is passed in between the gap of obstacles C_1 to C_2, and shear layers between the obstacles C_2 to C_5, just started to roll up in order to generate vortex shedding. However, the vortices are not generated completely in between the gap. The shed vortices, scattered form the rear ends of obstacles are shown irregularity in behavior and thus failed to form Von-Karman Vortex Street at downstream of channel. The distortion of vortices behind the obstacles clearly observed in Fig. 5(a, b). Due to incomplete generation of vortex shedding in between the obstacles, we named this flow mod as half developed irregular vortex shedding flow mod. Moreover, the vortices are no more round in shape as compared to Shear layer flow. With increase in gap spacing, strength and size of vortices also varied.

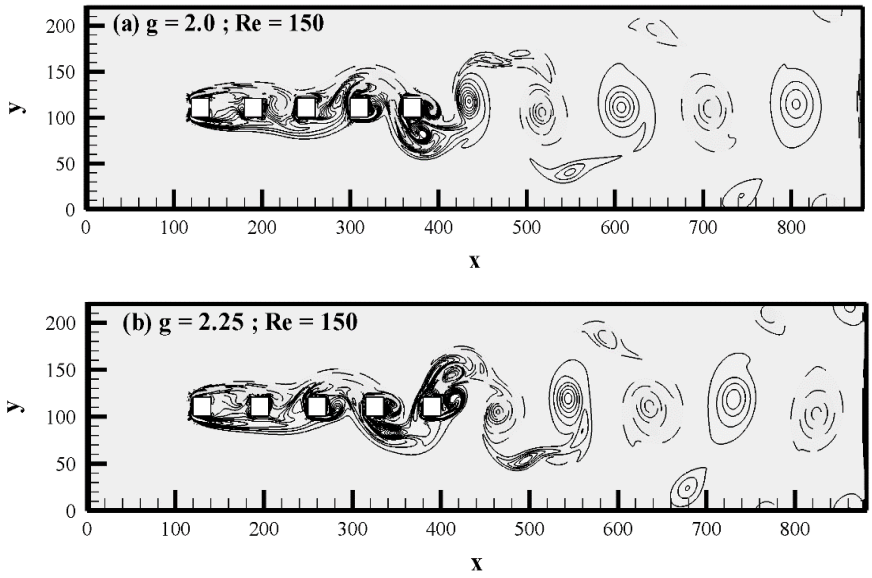

Fig 5(a-b). Vorticity contour for HDIVS flow mod.

The drag coefficients for HDIVS flow mod at g_c = 2.0, 2.5 at Re =150 is showing the periodic behavior (see Fig. 6). The magnitude of Cd_1 is smallest than that of drag coefficients of other selected obstacles. It is also seen from the Figure that C_2 having negative drag coefficient. The lift coefficients of obstacles C_1 and C_2 are contained periodic behavior but for obstacles C_3 to C_5, lift coefficient is modulated due to an irregular vortex shedding. The maximum amplitude of lift coefficient is found for obstacle C_5 and minimum for obstacle C_1.

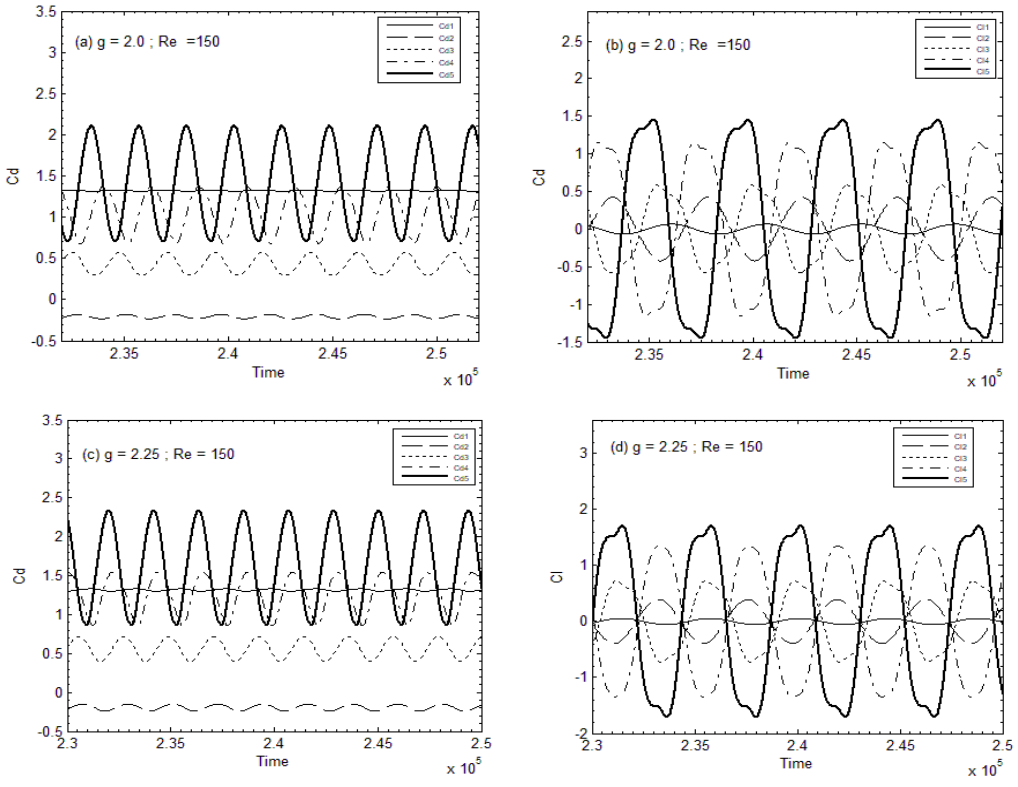

Fig 6(a-d). Drag and lift coefficients for HDIVS flow mod.

5.1.3. Fully developed two rows vortex shedding flow mod

The other existing flow mod is named as FDTRVS (fully developed two rows vortex shedding) flow mod observed at g_c = 2.5, 2.75, 3, 3.25 and 3.5 for fixed Reynolds number i.e. Re = 150 as shown in Fig. 7(a, b). In this flow mod, vortices are fully developed in between the gap of obstacles C_1-C_5 as well towards the down position of channel. The shed vortices behind the obstacle C_4, are changed into two rows after hitting the fifth obstacle. These two rows moved parallel to each other. Therefore, we called it fully developed two rows vortex shedding FDTRVS flow mod. When the indicated distance is less, the frequency generation of vortices is high and effected on size of vortices. Moreover the distance between two parallel rows of vortices at downstream of obstacles is decreased with increment in gap is represented in Fig. 7(c).

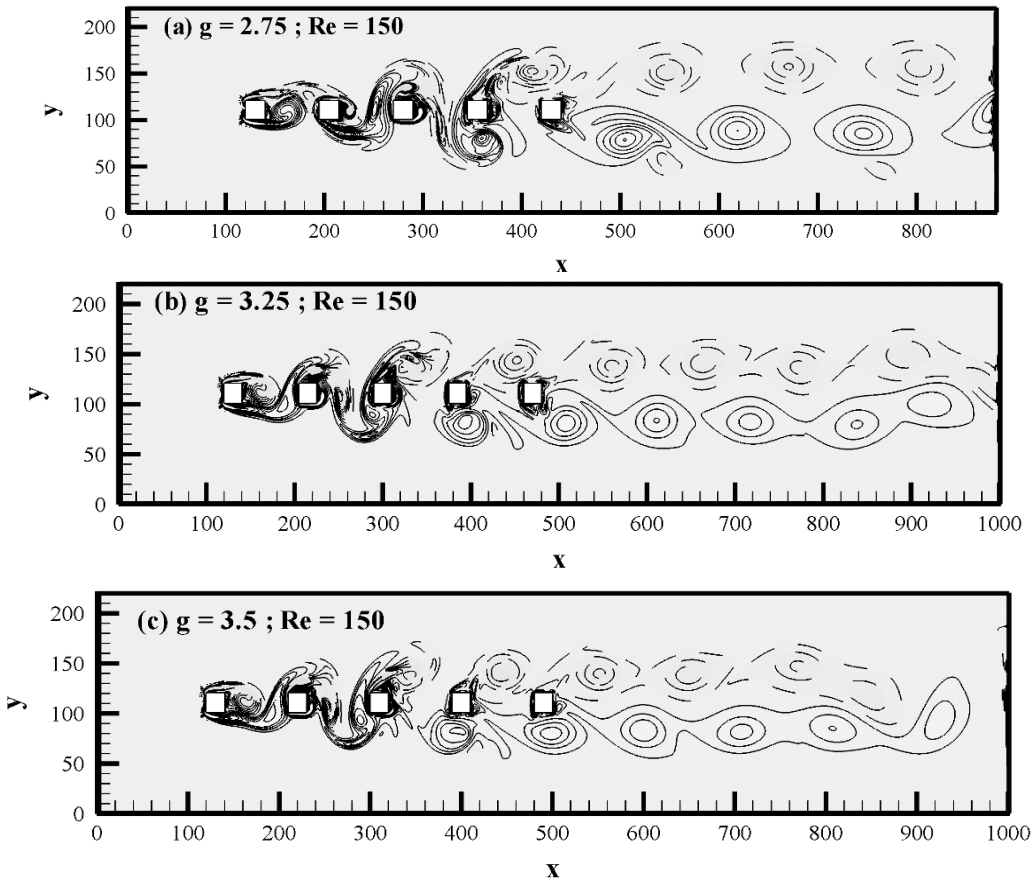

Fig 7(a-c). Vorticity contour for FDTRVS flow mod.

The drag coefficient at g_c = 2.75, 3.25 at Re =150 for FDTRVS flow mod is shown in Fig 8(a-d). It is observed that drag coefficients is shown almost the periodic behavior due to formation of fully developed vortices between the obstacles except for drag coefficient of obstacle C_4 at g_c = 2.75, which contained modulated behavior due to critical shape and size of vortices generated by obstacle C_4. The magnitude of drag coefficient for obstacle C_2 is maximum and the magnitude of obstacle C_5 is minimum for all observed case.

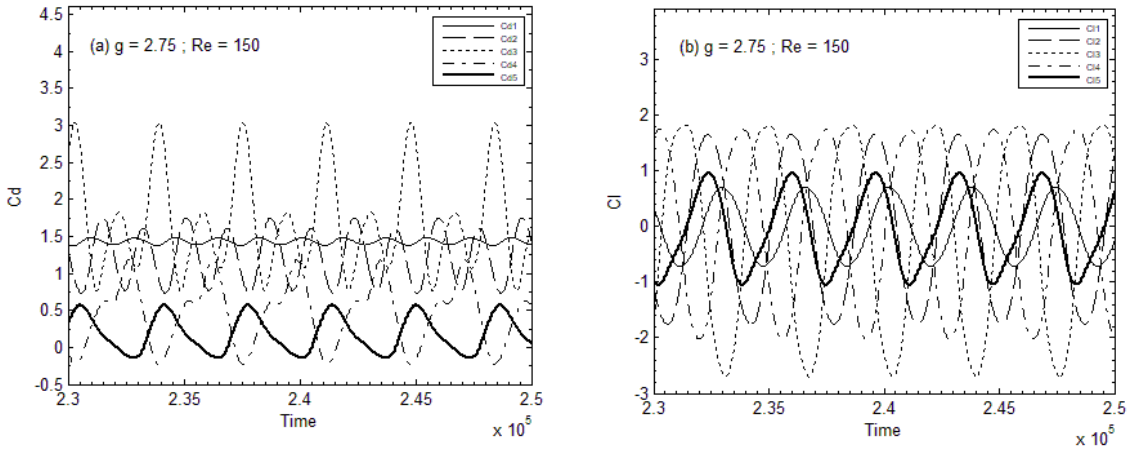

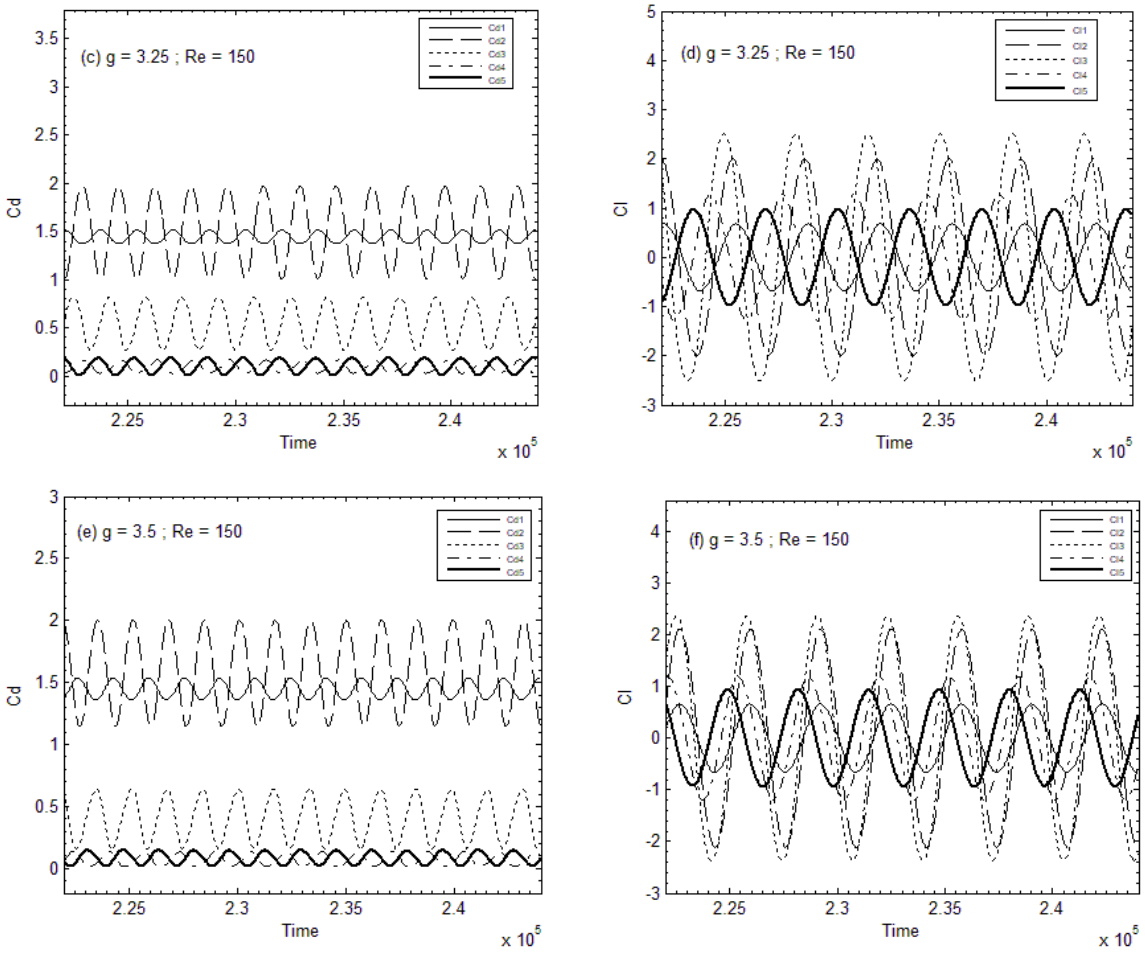

Fig 8(a-f). Drag and lift coefficients for FDTRVS flow mod.

The lift coefficients are showing periodicity, due to formation of regular vortex shedding at downstream of obstacles and their amplitude remained almost same with increase in gap spacing due to similar behavior of vortices. The maximum magnitude of lift coefficients is observed for obstacle C_3 and minimum for obstacle C_1.

5.1.4. Two rows single bluff body flow mod

The last flow mod is existed at large gap spacing i.e. g_c = 3.75, 4 and 5 at Re = 150. In this flow mod, shear layer rolled up in between the gap of obstacles C_1-C_2 and an alternate vortex shedding is found between the obstacles C_1-C_2 and C_2-C_3, but from obstacles C_3 –C_5, an alternate vortex shedding is transformed into two rows vortex shedding after hitting obstacle C_3. At some extent, these two rows moved parallel to each other, with opposite signs of shed vortices in the near wake. Moreover, the two parallel vortex rows did not persist for a long distance and started to merge with each other in form of single row at a downstream position of channel. We called this flow behavior as TRSBB (two rows single bluff body) (see Fig 9(a-b)). There is an irregularity in the shape and size of vortices. The size of vortices are decreased and strength increased with an increasing in the gap spacing.

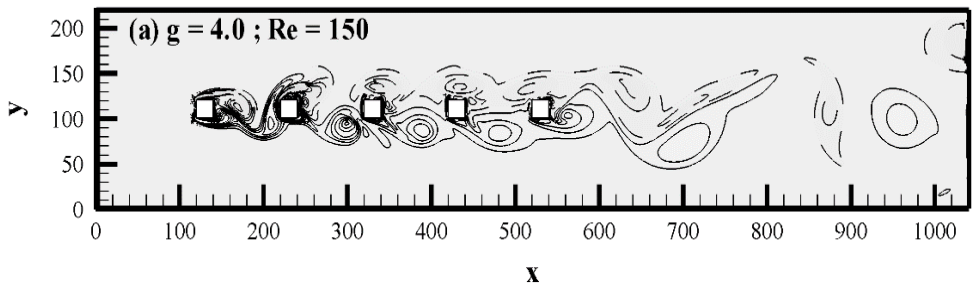

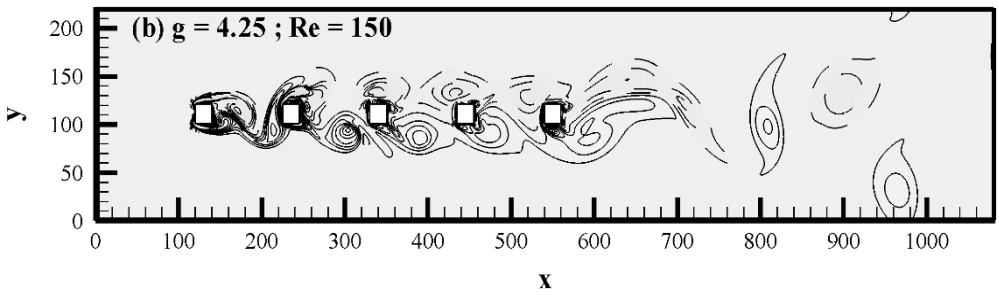

Fig 9(a-b). Vorticity contour for TRSBB flow mod.

The magnitude of drag coefficients for two rows single bluff body is periodic for the obstacles C_1-C_4, except for obstacle C_5 whose drag coefficient is modulated due to complicated structure of vortices generated at the end of obstacle C_5 as clear from Fig 10(a-d). It is noted that the amplitude for Cd_1 is larger and that of Cd_3 is smallest as compared to the Cd of other three remaining obstacles. The magnitude of Cl is periodic for all selected five obstacles due to same behavior of vortices at downstream position of obstacles. The obstacle C_2 is contained maximum value of lift coefficient and obstacle C_1 contained smallest value. The all existing flow mods at different values of g_c at Re = 150 are shown in Table 5.

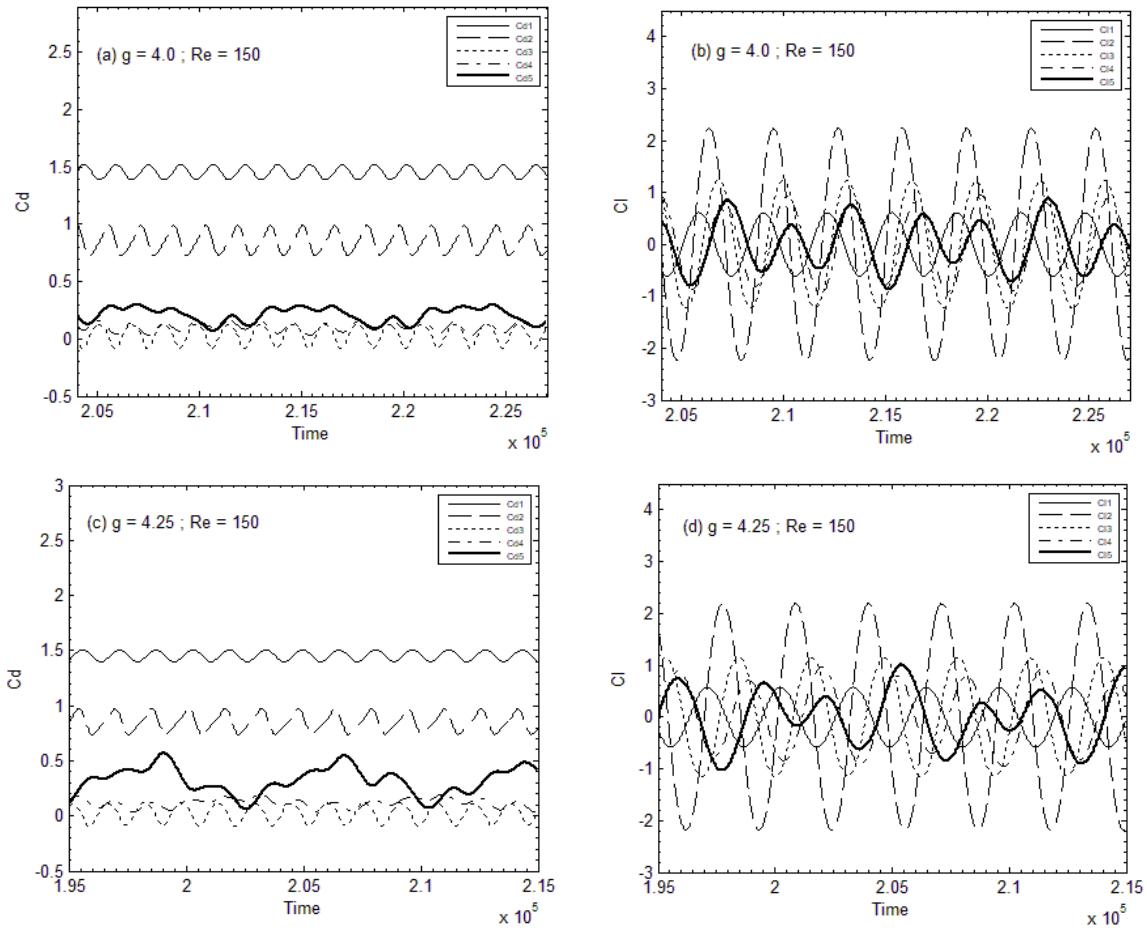

Fig 10(a-d). Drag and lift coefficients for TRSBB flow mod.

Table 5. Existing flow mods at g_c – 0.25 – 5

Gap spacing	Flow mods
g_c = 0.25, 0.5, 0.75, 1, 1.25, 1.5, 1.75	Shear layer reattachment flow mod (SLR)
g_c = 2, 2.25	Semi-developed irregular vortex shedding flow mod (FDIVS)
g_c = 2.5, 2.75, 3, 3.25, 3.5	Fully developed two rows vortex shedding flow mod (FDTRVS)
g_c = 3.75, 4, 5	Two rows single bluff body flow mod (TRSBB)

5.2. Force statistics

In physical parameters, the values Cd_{mean}, Cd_{rms}, Cl_{rms} and S_t are calculated against the various values of g with fixed values of Re = 150 (see Fig. 11(a-d)). The values of Cd_{mean} are represented in Fig. 11(a). The mean drag force of obstacle C_1 and C_2 having similar behavior. Their values are increased from g_c = 0.25 to 0.5, then declined in their values observed from g_c = 0.5

till 2.5. After that from g_c = 3 – 5, an increased in values of Cd_{mean} for obstacles C_1 and C_2 is occurred. An opposite behavior for obstacles C_3-C_5 is observed from the obstacles C_1 and C_2. The mean drag force values for C_3-C_5 is decreased from g_c = 0.25 - 0.5 and after that their values started to be increased from g = 0.5 – 3. At g > 3, mixed trend is observed for Cd_{mean} of obstacles C_3-C_5. The highest value of mean drag force is found at g = 5 for obstacle C_1 and it is 1.4594, while smallest value of Cd_{mean} is noticed for obstacle C_3 at g_c = 0.25. There may also seemed some negative values of Cd_{mean} for obstacle C_2 at g_c = 0.25 - 2.25 and for obstacle C_3 at g_c = 0.25 - 1.25 due to effect of thrust. The values of Cd_{rms} and Cl_{rms} against gap spacing are represented in Fig. 11(b, c) and they are representing mixed trend by increasing the values of gap spacing for all five selected obstacles. The largest value of Cd_{rms} reported at g_c = 5 for obstacle C_1, i.e. 0.7102, where existing flow mod is SBB flow mod. The smallest range of Cd_{rms} is investigated at g_c = 0.25 for C_2 and that is 0.00011. Here the existing flow mod is Shear layer flow mod. Similarly the maximum and minimum values for root men square values of lift coefficients are 1.6976 at g_c = 2.75 for obstacle C_3 and 0.00037 at g_c = 1.25 for obstacle C_1, respectively. Fig. 11(d) is drawn to represent the Strouhal number against gap spacing for obstacles C_1-C_5. The S_t values from g_c = 0.25 - 0.75 are increasing and then decreasing at values of g_c = 1 - 1.5. As gap spacing is increased from g_c = 1.75 – 5, the Strouhal number is again shown an increasing behavior continually. The greatest value of Strouhal number is examined at g_c = 5 for obstacle C_5, i.e. 0.1521. Where the flow mod is TRSBB. The smallest value of S_t is obtained at g_c = 1.5 for obstacle C_3 and that is 0.0862.

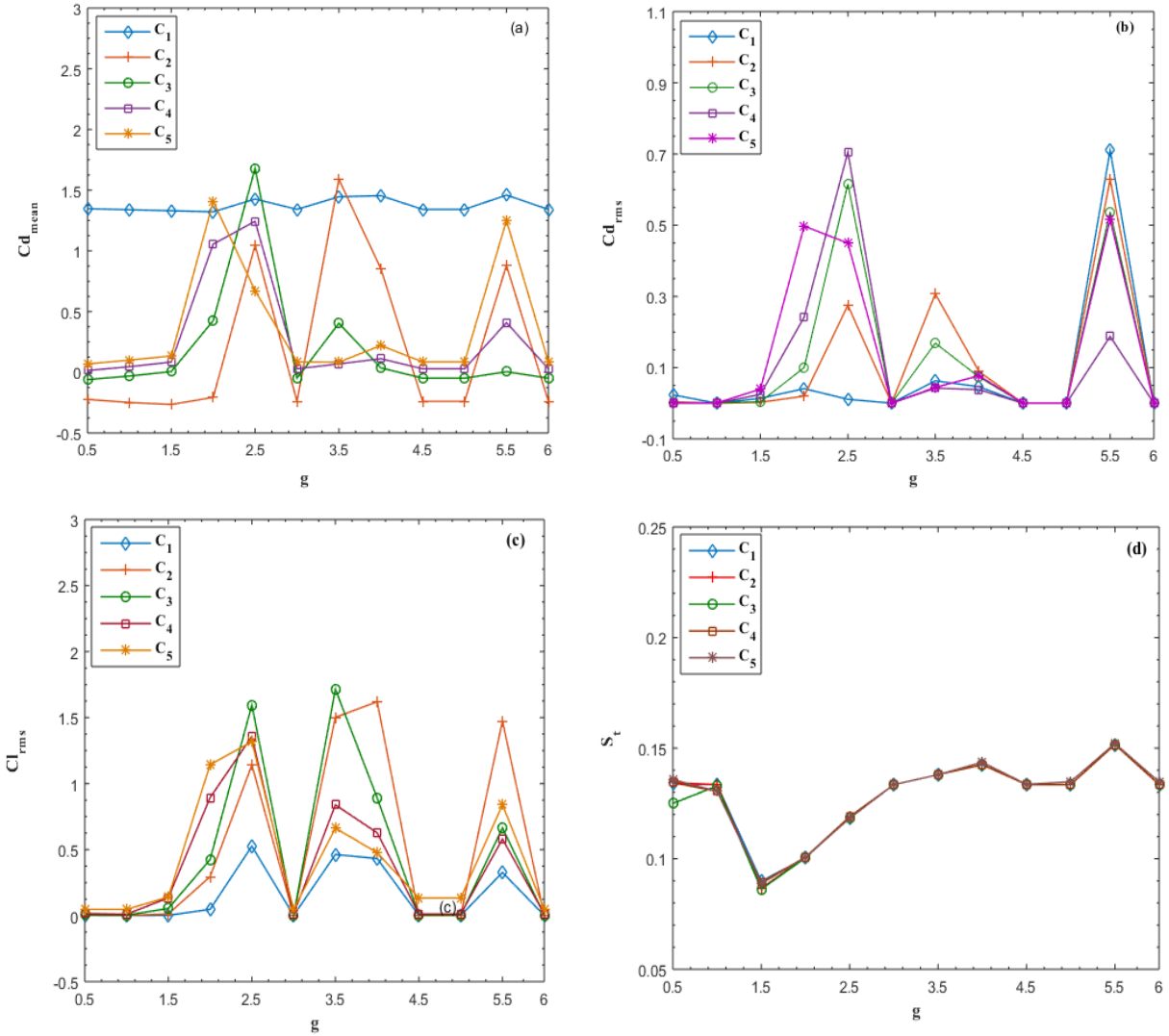

Fig 11. Change in values of (a) Cd_{mean} (b) Cd_{rms} (c) Cl_{rms} and (d) S_t with spacing g_c = 0.25-5 at Re = 150.

6. Conclusions

Two dimensional numerical simulation are conducted to find the effect of spacing ratio on variation of flow characteristics within the wake region and behind of the wake region in whole computational domain. This study was also conducted to examine the influence of gap ratios on force statistics for the flow around five aligned inline square obstacles of similar sizes. The numerical method used was the LBM. First of all the code validity was checked for the flow past a SS obstacle and obtained results were compared with results, those were available in literature, either experimental or numerical. Similar behavior were found among all the results. After that, numerical calculations were done for flow past five square obstacles placed in tandem arrangement. Important results obtained from this study are given below:

1. Four distinct kinds of flow mods were observed at g_c = 0.25 to 5 in this study. These are (a) Shear layer flow mod, (b) Hemi-developed irregular vortex shedding flow mod, (c) Fully developed two rows vortex shedding flow mod, (d) Two rows single bluff body flow mod.

2. The behavior of Cd_{mean} for obstacles C_1 and C_2 is quite different from obstacles C_3-C_5. The greatest value of Cd_{mean} is found at $g_c = 5$ for obstacle C_1 and it is 1.4594, while the minimum value of Cd_{mean} is for obstacle C_3 noted at $g_c = 0.25$.
3. There may also existed some negative values of Cd_{mean} for obstacle C_2 at $g_c = 0.25$ to 2.25 and for obstacle C_3 at $g_c = 0.25$ to 1.25 due to effect of thrust.
4. The largest range of Cd_{rms} and Cl_{rms} are obtained at gc = 5 for obstacle C_1 and at $g_c = 2.75$ for obstacle C_3, respectively.
5. The largest range of S_t is examined at $g_c = 5$ for obstacle C_5 and the smallest value of S_t is occurred at $g_c = 1.5$ for obstacle C_3 and that is 0.0862.

Conflict of Interest
The author declares no conflict of interest.

Funding Source
Not available

Data Availability Statement
Not applicable

References
1. P. Hishikar, S. K. Dhiman, A.K. Tiwari and V.K. Gaba, "Analysis of flow characteristics of two circular Obstacles in cross-flow with varying Reynolds number," Journal of Thermal Analysis and Calorimetry, 1-26, 2021.
2. M. Boland, S. Rashid, J. A. Esfahani and R. Masoodi, "Control of wake destructive behavior for different bluff bodies in channel flow by magneto-hydro-dynamics," The European Physical Journal Plus, 131 (6), 1-13, 2016.
3. F. Salwa, O. Fakher, and B. B. Brahim, "Influence of Various Staggered Arrangements of Square obstacles on the Drag and Lift Forces and the Wake Flow Behavior," International Journal of Fluid Mechanics Research, 48(6), 73–91, 2021.
4. F. Salwa, O. Fakher, and B .B. Brahim, "Identification of flow states around three staggered square obstacles at two symmetrical arrangements by a numerical investigation," International Journal of Modern Physics C, .31(11), 2050151, 2020.
5. F. Salwa Fezai, O. Fakher, B. C. Nader and B. B. Brahim, "Sensitivity of wake parameters to diameter Changes for a circular obstacle," International Journal of Modern Physics C, 29(11), 1850087, 2018.
6. Y. Zhou and M. W. Yiu, "Flow Structure, Momentum and Heat Transport in a two-tandem-obstacle Wake," Journal of Fluid Mechanics, 548, 17-48, 2006.
7. A. Sohankar and A. Etminan, "Forced convection heat transfer from tandem square obstacles in cross Flow at low Reynolds numbers," International Journal for Numerical Methods in Fluids, 60(7), 735-751, 2009.
8. G. Xu and Y. Zhou, "Strouhal numbers in the wake of two inline obstacles," Experiments in Fluids, 37, 248-256, 2004.
9. C. H. Liu and J. M. Chen, "Observations of hysteresis in flow around two square obstacles in a tandem arrangement," Journal of Wind Engineering and Industrial Aerodynamics, 90, 1019-1050, 2002.
10. A. Sohankar, "A numerical investigation of the flow over a pair of identical square obstacles in tandem Arrangement," International Journal for Numerical Methods in Fluids, 70, 1244-1257, 201
11. O. Inoue, M. Mori and N. Hatakeyama, "Aeolian tones radiated from flow past two square obstacles In tandem," Physics of Fluids, 18, 1-15, 2006.
12. X. Liu, "Wind loads on multiple obstacles arranged in tandem with effects of turbulence and surface roughness," Master Thesis, Graduate Faculty of the Louisiana State University and Agriculture and Mechanical College, 2003.
13. K. Tatsutani, R. Devarakonda and J.A.C Humphrey, "Unsteady flow and heat transfer for obstacle Pairs in a channel," International Journal of Heat and Mass Transfer, 13, 3311-3328, 1993.
14. T. Igarashi and K. Suzuki, "Characteristics of the flow around three circular obstacles arranged in line, "Bulletin of JSME, 27, 2397-2404, 1984.
15. A. B. Harichandan and A. Roy, "Numerical investigation of low Reynolds number flow past two and three circular obstacles using unstructured grid CFR scheme," International Journal of Heat and Fluid Flow, 31, 154–171, 2010.
16. K. Lam and S.C. Lo, "A visualization study of cross-flow around four obstacles in a square Configuration," Journal of Fluid and Structure, 6, 109-131, 1992.
17. P. P. Patil and S. Tiwari, "Numerical investigation of laminar unsteady wakes behind two inline square obstacles in a Channel," Engineering Application of Computational Fluid Mechanics, 3(3), 3, 369-385, 2009.
18. W. S. Abbasi, S. Ul. Islam, S.C. Saha, Y.T. Gu and Z.C. Ying, "Effect of Reynolds number on flow past four square obstacles in an-inline square configuration for different gap spacings," Journal of Mechanical. Science and Technology, 28(2), 539-552, 2014.
19. K. Lam and L. Zhou, "Experimental and numerical study for the cross-flow around four obstacles in an in-line square configuration," Journal of Mechanical. Science and Technology, 21, 1338-1343, 2007.
20. A.A. Hetz, M.N. Dhaubhadel and D.P. Telionis, "Vortex shedding over five in-line obstacles Journal of Fluid and Structure,5(3), 243-257, 1991.
21. C.M. Sewatkar, R. Patel, A. Sharma and A. Agrawal, "Flow around six in-line Square obstacles,"Journal of Fluid Mechanics, 710, 195-233, 2012.
22. Y. Bao, Q. Wu and D. Zhou, "Numerical investigation of flow around an inline square obstacle array with different spacing ratios," Computers & Fluids, 55, 118-131, 2012.
23. A. A. Mohammad, "Lattice Boltzmann Method: Fundamentals and Engineering Applications with Computer Codes,

Springer, 2011.
24. D. A. Wolf-Gladrow, "Lattice-Gas Cellular Automata and Lattice Boltzmann Method-An Introduction," Springer, 2005.
25. P. L. Bhatnagar, E.P. Gross and M. Krook, "A model for collision processes in gases. I. Small amplitude processes in charged and neutral one-component system," Physical Review, 94, 511-525, 1954.
26. Y. Qian, D. d'Humieres and P. Lallemand, "Lattice BGK models for Navier-Stokes Equation," Europhys Letter, 17(6), 479-484, 1992.
27. Z. Guo, H. Liu, L.S. Luo and K. Xu, "A comparative study of the LBE and GKS method for 2D near Incompressible laminar flows," Journal of Computational Physics, 227, 4955-4976, 2008.
28. D. Yu, M. Renwei, L. S. Luo and S. Wei, "Viscous flow computations with the method of lattice Boltzmann equation," Progress in Aerospace Sciences, 39, 329-367, 2003
29. M. A. Gallivan, D. R. Noble, J. G. Georgiadis, R. O. Buckius, "An evaluation of the bounce-back boundary condition for lattice Boltzmann simulations," International Journal for Numerical Methods in Fluids. 25(3), 249–263, 1997.
30. Okajima, "Strouhal numbers of rectangular obstacles," Journal of Fluid Mechanics, 123, 379-398, 1982.
31. R. W. Davis and E. F. Moore, "A numerical study of vortex shedding from rectangles," Journal of Fluid Mechanics, 116, 475-506, 1982.
32. S. Malekzadeh and A. Sohankar, "Reduction of fluid forces and heat transfer on a square obstacle a laminar flow mod using a control plate," International Journal of Heat and Fluid Flows, 34,15-27, 2012.
33. J. Robichaux, S. Balachandar and S.P. Vanka, "Three-dimensional floquet instability of the wake of a square obstacle," Physics of Fluids, 1, 560-578, 1999.
34. P. K. Gera and R. K. Sharma, "CFD analysis of 2D unsteady flow around a square obstacle, International Journal of Applied Engineering and Research Dindigul, 1(3), 602-610, 2010.
35. A.S. Abograish and A.E. Alshayji, "Reduction of fluid forces on a square obstacle in a laminar flow Using passive control methods," COMSOL Conference, Boston, USA, 2013.